Locking of a passive Q-switched chaotic laser system to a small external modulation

Takayuki Tsukamoto, Maki Tachikawa, and Toshiki Sugawara*
Department of Physics, University of Tokyo, 7-3-1 Hongo, Bunkyo-ku, Tokyo 113, Japan

Tadao Shimizu
Department of Physics, Science University of Tokyo, 1-3 Kagurazaka, Shinjuku-ku, Tokyo 162, Japan
(Received 4 January 1995)

We find that a CO_2 laser oscillation can be transferred from the chaotic state into the periodic pulsation state by introducing a small-amplitude sinusoidal modulation on an intracavity absorption. The proposed rate-equation model successfully reproduces these characteristic behaviors of the laser system. The numerical calculations based on the present model predict that the periodic window on the bifurcation diagram as a function of a normalized intracavity absorption coefficient shifts in two ways by the modulation: towards the lower absorption side when $T < T_0$ and towards the higher absorption side when $T > T_0$, where T_0 is the period of the laser pulsation in the window without the modulation and T is the period of the modulation. In the windows the laser pulsation is locked to the modulation signal, but the relative phase between them is different by π in the two cases stated above.

PACS number(s): 42.50.Ne, 42.60.Fc, 42.55.Lt, 05.45.+b

I. INTRODUCTION

Chaos has been extensively studied in numbers of physical systems as a fundamental phenomenon inherent in nonlinear processes. Recently, a great effort has been made to open a new way of utilizing chaos in practical applications, such as signal processing, neural networks, and control of chemical and biological systems [1–4]. The dynamical behavior in a chaotic system changes drastically, depending sensitively on system parameters or initial conditions. Therefore a variety of temporal variations can be obtained with only a small perturbation of the dynamical system.

So far, several methods have been proposed to lock a chaotic system to one of the unstable periodic orbits embedded within the strange attractor. In the method developed by Ott, Grebogi, and Yorke (the OGY method), a time-dependent perturbation, which is a function of the deviation from the desired orbit in the phase space, is fed to an accessible parameter [1]. Since the correction signal needs to be calculated in response to the system dynamics, the applicability of this method to fast systems is limited by the speed of the feedback loop, usually that of a digital-to-analog or an analog-to-digital converter.

On the other hand, Lima and Pettini suggested that a weak periodic modulation of a system parameter may convert the chaotic motion to a periodic one [3]. This effect was verified in several systems, such as a driven dumped pendulum [4] and a magnetoelastic beam [5]. Compared with the OGY method, this method is simple and easily applicable to relatively fast systems, such as lasers and electronic devices. Recently, Meucci *et al.* employed this technique to stabilize an unstable periodic pulsation of a chaotic laser whose cavity loss was periodically modulated by an electro-optic device [6].

A single-mode laser which contains a saturable absorber inside its cavity exhibits self-induced pulsation, known as passive Q switching (PQS) [7]. In a CO_2 laser, chaotic PQS pulsation appears in some limited region of the parameters [8,9]. The purpose of this paper is to demonstrate that the chaotic PQS pulsation of a CO_2 laser can be converted to periodic ones by application of weak periodic modulation on the absorption. The response of the laser is investigated extensively as a function of the amplitude and frequency of the modulation on the basis of the rate-equation model.

II. EXPERIMENT

The experimental setup is described in detail in Ref. [10]. In brief, the CO_2 laser consists of a 2.1-m-long gain tube and a 35-cm-long intracavity absorption cell. The total cavity length is 3.5 m. A gas mixture of CO_2, N_2, and He (1:1:8) flows through the laser tube at a total pressure of 12.0 Torr. The laser oscillates on a single mode of TEM_{00} at the 9 μm $R(18)$ line.

The intracavity cell contains gaseous saturable absorber (HCOOH) and buffer gas (SF_6) at 7 mTorr and 270 mTorr, respectively. The absorption coefficient of the saturable absorber is controlled by applying dc and ac voltages to the Stark electrodes in the cell. The electrodes consist of two aluminum-coated glass plates which are placed parallel to each other. Each electrode has a dimension of 9.5 cm in length and 3.5 cm in width. The

*Present address: Central Research Laboratory, Hitachi Ltd., 1-280 Higashikoigakubo, Kokubunji-shi, Tokyo 185, Japan.

gap between the electrodes is 1.0 cm.

Figure 1 shows the chaotic pulse train [(a)], the power spectrum [(b)], and the return map [(c)] observed when only dc voltage of 38 V is applied to the Stark electrodes. The first return map is constructed by plotting the $(n+1)$th peak height in the pulse train as a function of the nth peak height. This system is characterized by a one-dimensional unimodal return map.

The dependence of the observed PQS behavior on the amplitude of the sinusoidal modulation is shown in Fig. 2. The modulation period is fixed at 104 μs. In the middle column are depicted the Lissajous maps where the laser intensity is plotted as a function of the instantaneous voltage of the ac Stark component. This is a good measure to observe locking of the chaotic system to the external modulation. The chaotic pulsation is locked to the external modulation at the modulation amplitude of 350 mV. The Lissajous map of the closed loop clearly shows this evidence. The resolution of the power spectrum is not good because of the limited number of data points in the time sequence, but the spectrum shows a peak at the modulation frequency [Fig. 2(c)]. It is noted that six spikes form a period. At larger or smaller modulation amplitude, the laser oscillation is not locked to the Stark modulation but stays in chaos. The achievement of the experiment was very sensitive to external noise. Special care has been taken to remove the external noise, such as fluctuation of the discharge current, the vibration from the floor, the acoustic perturbation, and so on. However, some "intrinsic" noise may not be removed thoroughly and the chaos-locking transition is not clearly observed in the experimental power spectra.

A similar dependence is also observed when the modulation period is 82.5 μs (Fig. 3). The chaotic pulsation changes into a periodic one at a modulation amplitude of 770 mV. In this case, however, five spikes are involved in a period.

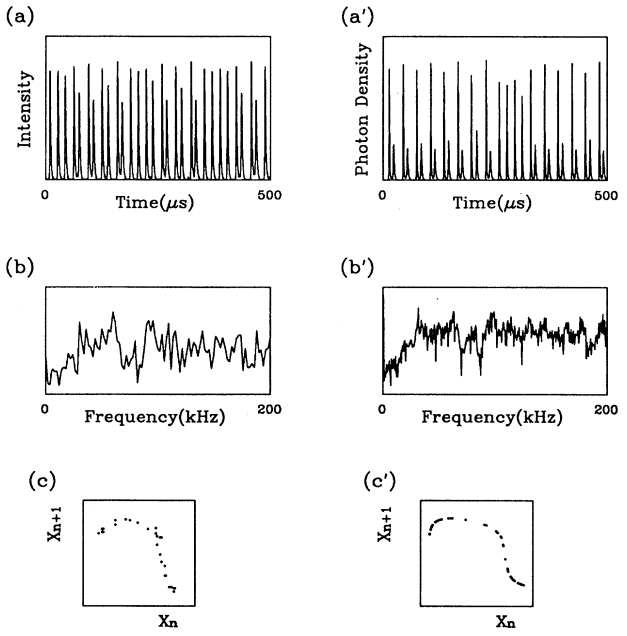

FIG. 1. Typical examples of the observed and the calculated chaotic PQS pulse trains [(a) and (a'), respectively], their power spectra [(b) and (b')], and first return maps [(c) and (c')] in the absence of periodic modulation.

III. THEORETICAL DISCUSSION

The rate-equation analysis is carried out based on the three-level:two-level model, in which the gain medium is represented by three vibrational levels, and the absorption medium is described by two levels [9]. The relevant difference of the present model from those described in Ref. [7] is that in the present case the lower vibrational level of the gain medium has a two orders of magnitude higher relaxation rate than the upper level [10]. So far this model has been successfully applied to reproduce with detailed fidelity the observed characteristic behaviors of CO_2 lasers with saturable absorbers [8,11]. According to the model, the dynamics of the laser system is described by the following set of differential equations for the population densities in the upper and lower laser levels, M_1 and M_2, the difference in the population density between the upper and lower rotational-vibrational states of the saturable absorber, N, and the photon density in the lasing mode, I:

$$\dot{I} = B_g f_g(J) I(M_1 - M_2) l_g/L - B_a I N l_a/L - kI, \quad (3.1)$$

$$\dot{M}_1 = -B_g f_g(J) I(M_1 - M_2) + P(M - M_1 - M_2) - (R_{10} + R_{12}) M_1, \quad (3.2)$$

$$\dot{M}_2 = B_g f_g(J) I(M_1 - M_2) + R_{12} M_1 - R_{20} M_2, \quad (3.3)$$

$$\dot{N} = -2B_a I N - r(N - N^*), \quad (3.4)$$

where B_g and B_a are the cross section multiplied by the light velocity c for the induced emission in the gain medium and the absorption in the absorbing medium, respectively. The lengths of the gain tube, the absorption cell, and the laser cavity are denoted as l_g, l_a, and L, respectively. The fraction of CO_2 molecules in the rotational level with the quantum number J is represented by $f_g(J)$, the cavity loss rate by k, and the pumping rate by P. The relaxation rate from the i level to the j level in the laser medium is written as R_{ij} (the ground state is denoted by 0), and r is the collisional relaxation rate of the absorbing gas. The population density of CO_2 molecules is denoted by M, and the thermal equilibrium value of N by N^*.

In the present case, the absorption rate B_a is sinusoidally modulated by the Stark effect, so the parameter B_a is expressed as

$$B_a = B_a^*[1 + \alpha \cos(2\pi t/T)], \quad (3.5)$$

where α and T are the amplitude and the period of the modulation, respectively. B_a^* is the value of the absorption rate in the absence of modulation.

Figures 1(a'), 1(b'), and 1(c') show the chaotic pulse

TABLE I. Parameters used in the numerical analysis.

k	2.37 MHz	R_{10}	947.8 Hz	R_{20}	360.2 kHz
R_{12}	19.0 Hz	$B_g M f_g(J) l_g/L$	4075.6 MHz	r	7.152 MHz
$B_a^* N^* l_a/L$	3.314 MHz	$B_a^*/[B_g f_g(J)]$	293.9	P	61.6 Hz

train, the power spectrum, and the return map, which are numerically calculated with Eqs. (3.1)–(3.4) in the absence of periodic modulation ($\alpha = 0$). General features of the observed PQS dynamics, such as the pulse form, the repetition rate, and the unimodal return map, are well reproduced with the reasonable values of the parameters for the present laser system in Table I [10,11].

A global feature of the bifurcation diagram in the absence of periodic modulation is shown in Fig. 4 where the calculated peak values of the pulse train are plotted as a function of B^*, where B^* is a normalized parameter proportional to the absorption as $B^* \equiv B_a^* N^* l_a/L$. There are the periodic windows associated with six and five peak values around B^*=3.306 MHz and 3.334 MHz, respectively.

The observed PQS pulse trains, the Lissajous maps, and the power spectra shown in Figs. 2 and 3 are well reproduced by the calculation as a function of α as shown in Figs. 5 and 6, respectively. The value of B^* is fixed at 3.314 MHz which is fairly close to those of the windows stated above. In both cases, the laser output is locked to the external modulation in a limited range of α. It is noted that the locked state of Fig. 5(c) involves six spikes in a period (period-6 state) while the state of Fig. 6(d) involves five (period-5 state). The value of the applied field in mV corresponding to each value of α is evaluated from the following relation and shown in the caption of Figs. 5 and 6. In our experiment, the ac Stark voltage is so small that a change in the absorption rate is almost a linear function of it and $\Delta B_a/B_a = 3.8 \times 10^{-4}$ at $\Delta V_{ac} = 100$ mV.[1] The theoretically predicted modulation amplitudes and the observed ones to lock the chaotic

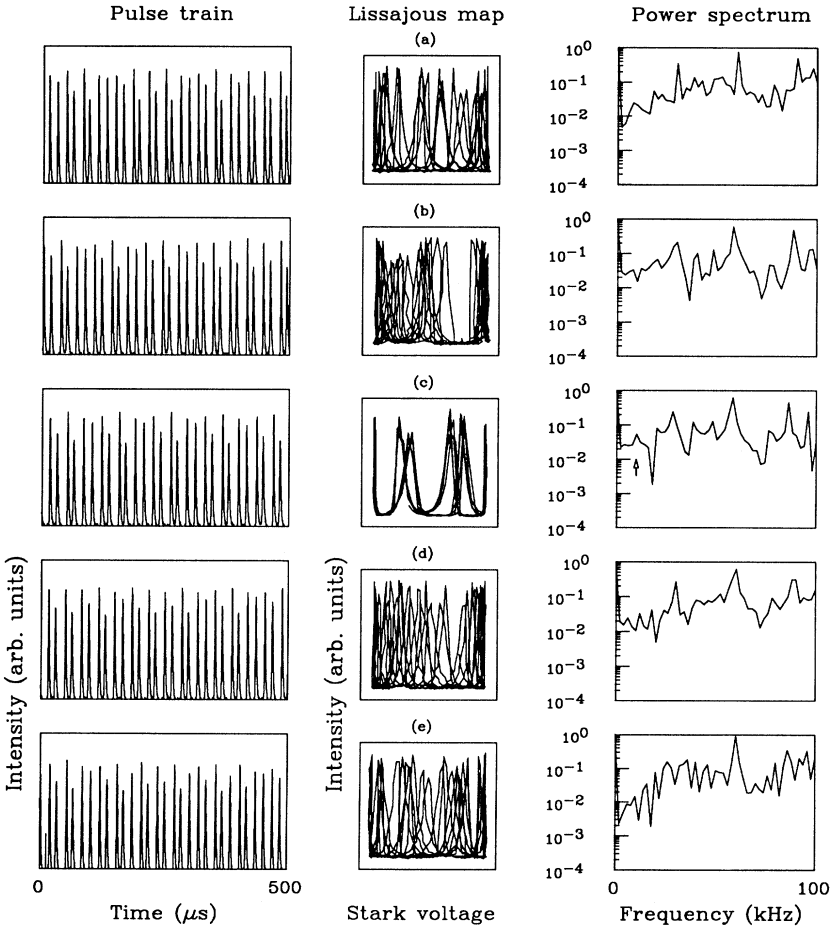

FIG. 2. Observed dependence of the PQS pulse train with its Lissajous map and power spectrum on the modulation amplitude when the modulation period is 104 μs. The applied modulation voltages are (a) 40 mV, (b) 300 mV, (c) 350 mV, (d) 400 mV, and (e) 780 mV. The modulation frequency is indicated by an arrow.

[1]This is derived from the numerical plot of the change of absorption due to the Stark shift of the relevant energy levels of HCOOH [12].

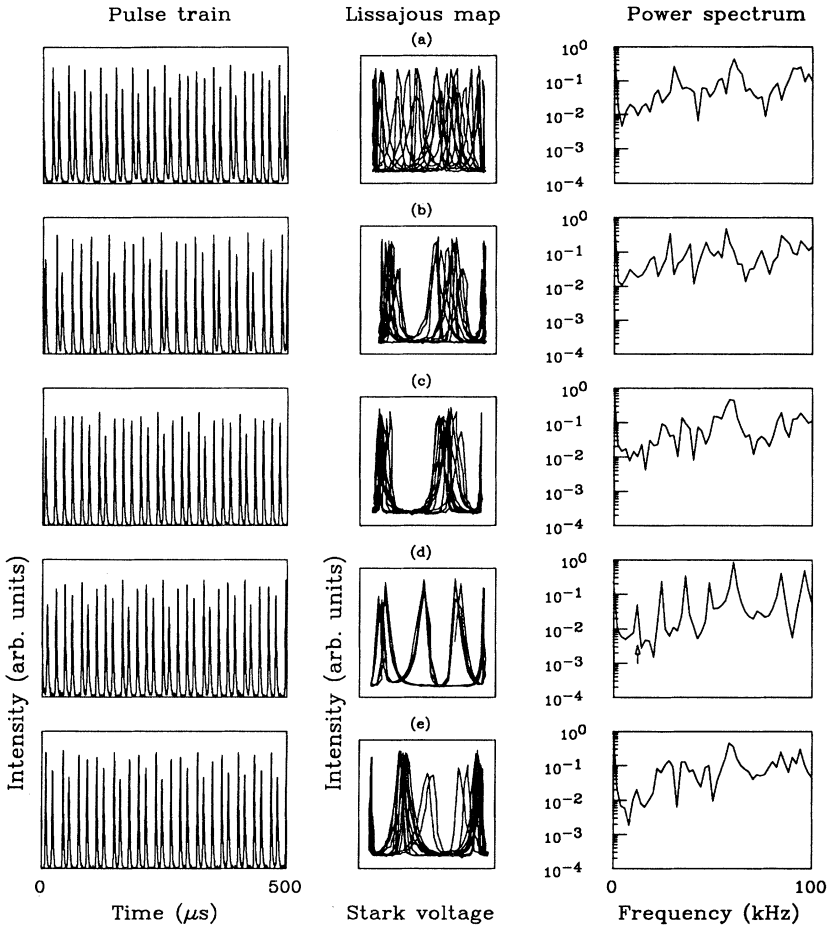

FIG. 3. Observed dependence of the PQS pulse train with its Lissajous map and power spectrum on the modulation amplitude when the modulation period is 82.5 μs. The applied modulation voltages are (a) 40 mV, (b) 360 mV, (c) 640 mV, (d) 770 mV, and (e) 900 mV. The modulation frequency is indicated by an arrow.

state to the periodic ones are in good quantitative agreement.

The phenomenon of frequency locking is investigated in more detail by numerical analysis. The parameter regions for the period-5 and -6 states are quite limited as shown in the phase diagram of Fig. 7. It is noted that the locking occurs only when the modulation period is close to those of the laser pulsations in the periodic windows in the absence of the modulation.

Figure 8(a) shows the enlarged version of the bifurcation diagram around the periodic window with five peak values in the absence of modulation. When T (the period of the modulation signal) is close to T_0 (that of the periodic laser pulsation in the absence of the modulation), the periodic window shifts in two ways as a function of modulation amplitude as shown in Figs. $8(b_1)$–$8(b_4)$ and $8(c_1)$–$8(c_4)$. When $T < T_0$, the window shifts towards the lower absorption (the lower branch), and when $T > T_0$ it shifts towards the higher absorption (the higher branch). For a given value of α, the width of the window is slightly dependent on T. The value of T at the maximum width of the window is defined by T_{opt}^{-} for the lower branch and by T_{opt}^{+} for the higher branch. It is

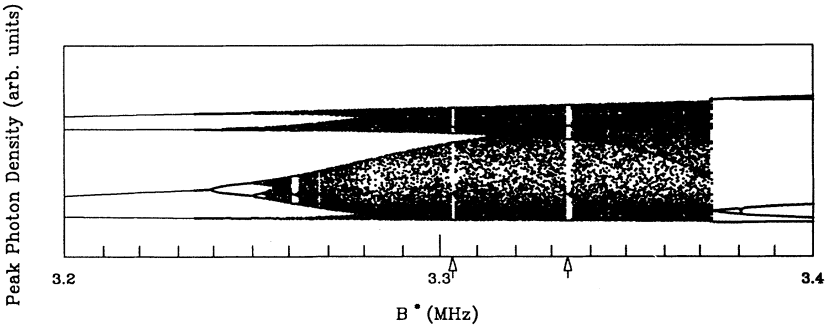

FIG. 4. Bifurcation diagram calculated as a function of B^* when there is no periodic modulation. There are periodic windows, which are indicated by the arrows, with six and five different peak heights at B^*=3.306 and 3.334 MHz, respectively.

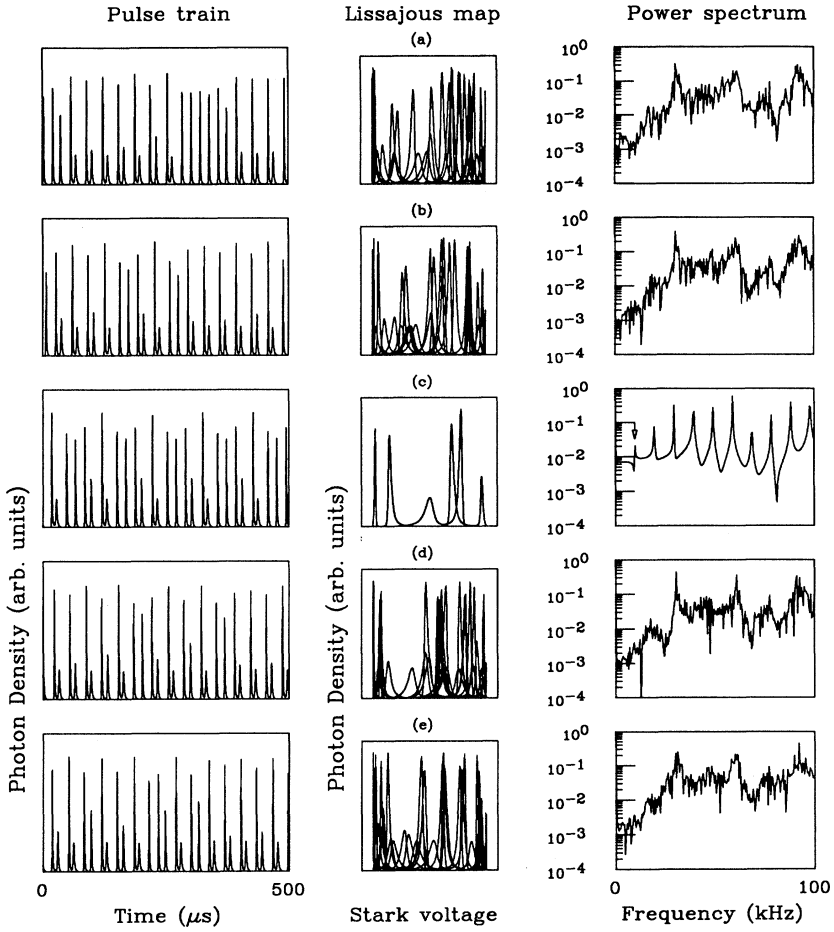

FIG. 5. Calculated dependence of the PQS pulse train with its Lissajous map and power spectrum on the modulation amplitude when the modulation period is 102.2 μs. The modulation amplitudes α and corresponding ac Stark voltage are (a) 0.016%, 42 mV, (b) 0.12%, 320 mV, (c) 0.14%, 370 mV, (d) 0.16%, 420 mV, and (e) 0.31%, 820 mV. The modulation frequency is indicated by an arrow.

found that $T_{opt}^{\pm}$ is expressed by the simple relation of $T_{opt}^{\pm} \simeq T_0(1 \pm \alpha)$ as shown in Fig. 9.

The shift of the window in both branches is quite large as compared with the width of the window and the modulated window appears even in the regions of unmodulated periodic pulsation that are outside the chaotic region shown in Fig. 4 [Figs. 8(b_3) and 8(c_3)].

Figure 10 shows the phase relation between the modulation signal and the laser pulsation locked to the modulation. It is found that the relative phase of the periodic pulsation against the modulation signal differs by π between the lower and higher branches.

The position of the window is defined by B_m^* which is the value of B^* at the right end of the window in the presence of modulation with $T_{opt}^{\pm}$. B_0^* is the position of the window in the absence of the modulation. The amount of the shift of the window is denoted by $\Delta B^* \equiv B_m^* - B_0^*$. Figure 11(a) shows the shift of the window normalized by B_0^* as a function of the modulation amplitude α. It is found that ΔB^* is proportional to α in both branches and $\Delta B^*/B_0^*$ is well expressed by $\Delta B^*/B_0^* \simeq \pm 2.0\alpha$, where the sign + corresponds to the higher branch and the sign − to the lower branch.

Figure 11(b) shows the width of the window in the presence of the modulation normalized by that in the absence of the modulation as a function of the modulation amplitude α. It is found that the normalized width is expressed by a linear function of α in each branch. In the higher absorption branch the width increases linearly with an increase of α, but the value extrapolated to $\alpha = 0$ is not on the linear relation. In the lower absorption branch, on the other hand, the width of the window decreases linearly with α.

The characteristic features of the present chaotic system for small-amplitude modulation will be summarized as follows: (1) a two-way shift of the periodic window, (2) a phase difference by π between the two branches, (3) a linear dependence of the shift on the modulation amplitude, and (4) a linear dependence of the window width on the modulation amplitude. Although the physical interpretation of these issues for the present laser system is not easy, the characteristic features of (1)–(3) can be shown in the analysis of a simpler model of the discrete quadratic map (the modified logistic map) as shown in the Appendix. Cicogna and Fronzoni reported similar features to the issues (1) and (3) in the motion in a

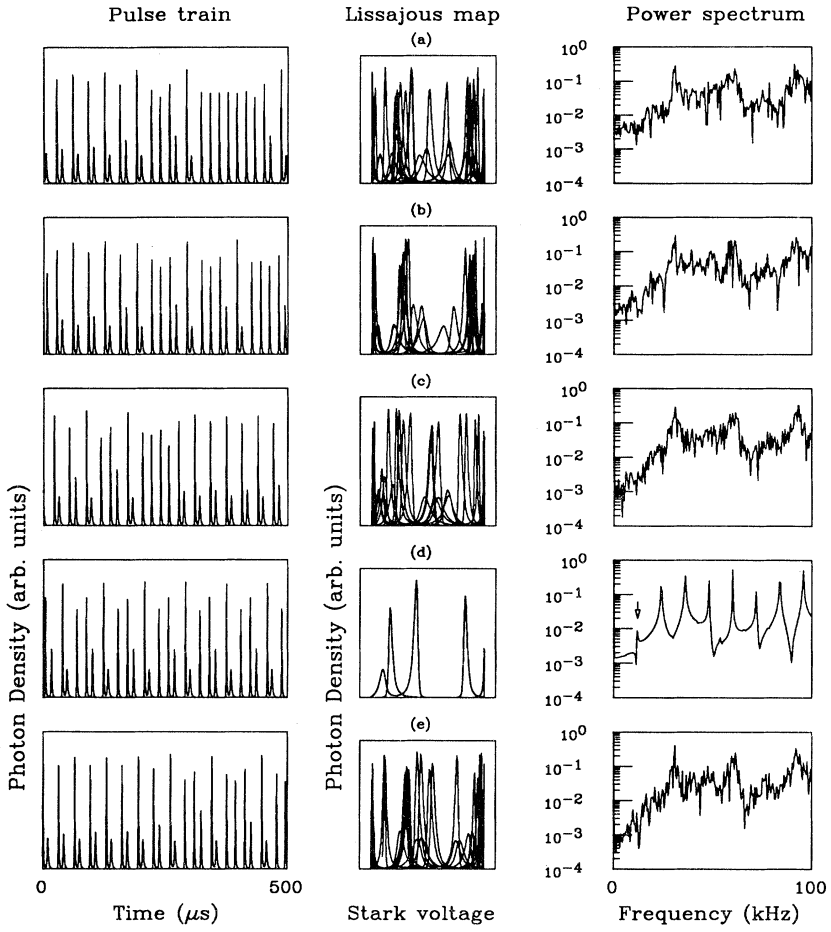

FIG. 6. Calculated dependence of the PQS pulse train with its Lissajous map and power spectrum on the modulation amplitude when the modulation period is 83.8 μs. The modulation amplitudes α and corresponding ac Stark voltage are (a) 0.016%, 42 mV, (b) 0.14%, 370 mV, (c) 0.25%, 660 mV, (d) 0.31%, 820 mV, and (e) 0.35%, 920 mV. The modulation frequency is indicated by an arrow.

bistable Duffing-Holmes potential where the threshold of the chaos depends linearly on the modulation amplitude [13].

IV. CONCLUSION

It has been demonstrated experimentally and theoretically that a chaotic PQS pulsation in a CO_2 laser can be transferred to periodic ones by weak periodic modulation of the saturable absorber. The rate-equation analysis has revealed that the periodic window on the bifurcation diagram as a function of a normalized absorption coefficient shifts in two ways on modulation with period T which is close to T_0 (that of the periodic laser pulsation in the window of the unmodulated system). The shift is towards the lower absorption side when $T < T_0$ (the lower branch) and towards the higher absorption side when $T > T_0$ (the higher branch). In the window the laser pulsation is locked to the modulation signal, but the relative phase between them is different by π in the two branches.

Since the chaotic system has an infinite number of periodic windows, the present method is applicable to produce a variety of periodic optical signals without large

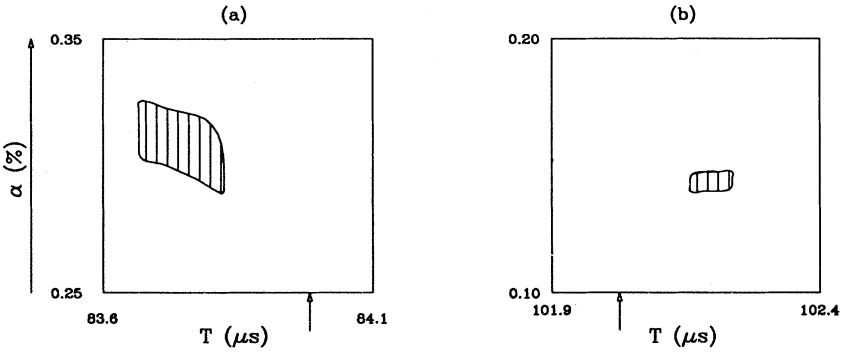

FIG. 7. Calculated phase diagrams of the amplitude and the period of the modulation for (a) the period-5 state and (b) the period-6 state when B^* is 3.314 MHz. The locking occurs in the hatched areas. The period of the pulsation in the periodic windows without modulation is indicated by the arrows.

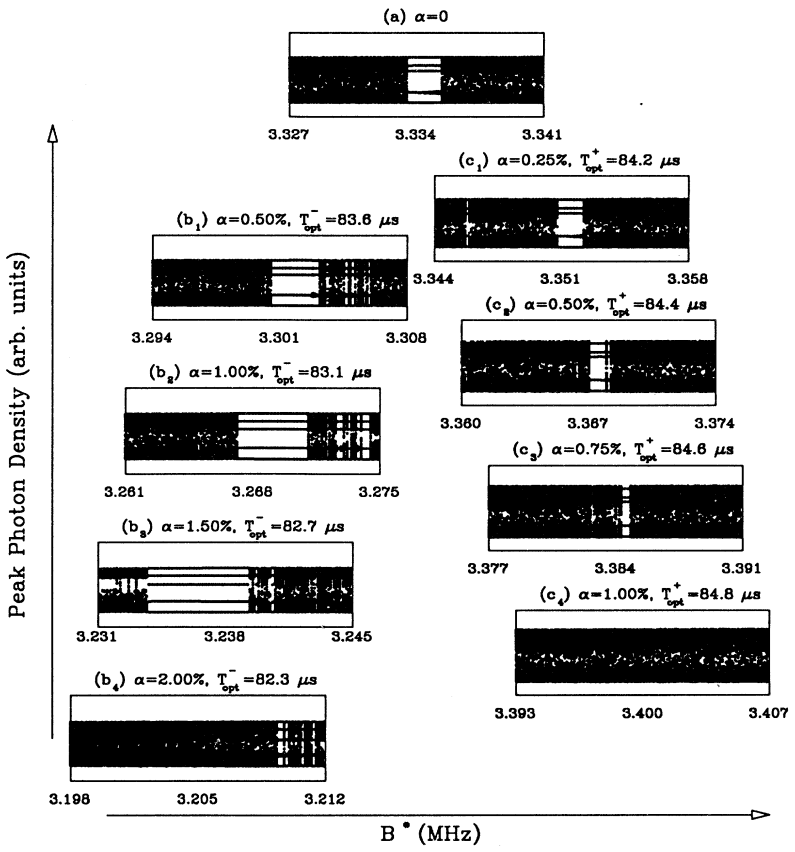

FIG. 8. Calculated shift and broadening (narrowing) of the periodic window with five peaks as a function of the modulation amplitude. The amplitudes and periods are (a) $\alpha = 0$, (b_1) $\alpha = 0.50\%$, $T^-_{opt} = 83.6$ μs, (b_2) $\alpha = 1.00\%$, $T^-_{opt} = 83.1$ μs, (b_3) $\alpha = 1.50\%$, $T^-_{opt} = 82.7$ μs, (b_4) $\alpha = 2.00\%$, $T^-_{opt} = 82.3$ μs, (c_1) $\alpha = 0.25\%$, $T^+_{opt} = 84.2$ μs, (c_2) $\alpha = 0.50\%$, $T^+_{opt} = 84.4$ μs, (c_3) $\alpha = 0.75\%$, $T^+_{opt} = 84.6$ μs, and (c_4) $\alpha = 1.00\%$, $T^+_{opt} = 84.8$ μs.

modification of the system parameters. Also, the feature that the width of the window increases with an increase of the amplitude in the lower branch makes it easier to realize the periodic pulsation which is available in a very restricted region of the absorption coefficient in the absence of modulation.

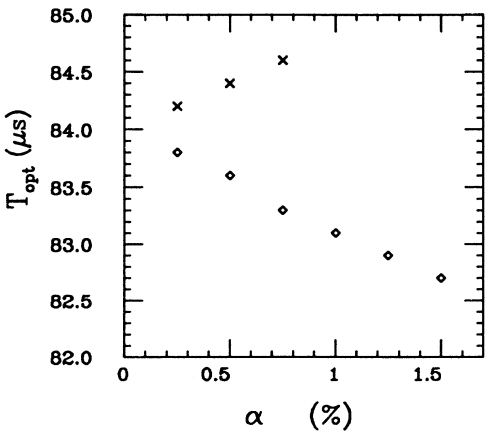

FIG. 9. $T^{\pm}_{opt}$ as a function of the modulation amplitude α. $\diamond$ and $\times$ represent the lower and the higher branch, respectively.

ACKNOWLEDGMENT

We greatly acknowledge Professor T. Kuga, University of Tokyo, for stimulating comments on the present work.

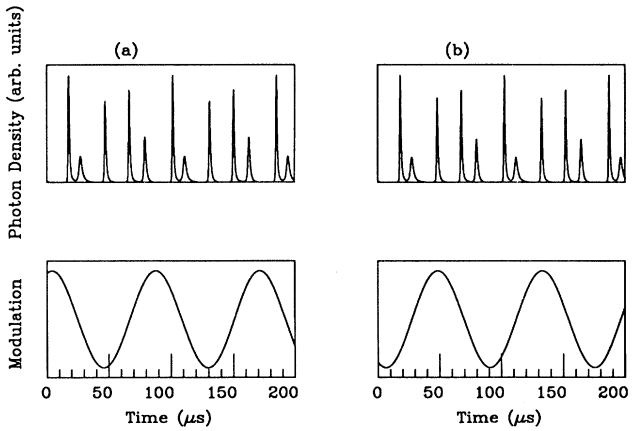

FIG. 10. Calculated relation between the modulation signal and the periodic laser pulsation in the two branches. The modulation parameters are (a) $\alpha = 0.50\%$, $T^-_{opt} = 83.6$ μs (the lower branch), and (b) $\alpha = 0.50\%$, $T^+_{opt} = 84.4$ μs (the higher branch).

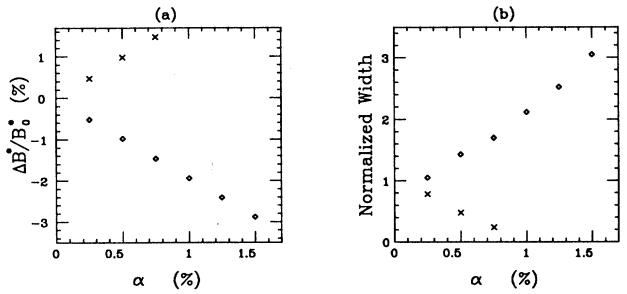

FIG. 11. (a) Calculated shift of the window in the presence of modulation as a function of the modulation amplitude α. (b) Calculated width of the window in the presence of modulation as a function of α based on the numerical calculation. In both figures, $\diamond$ and $\times$ represent the lower and the higher branch, respectively.

APPENDIX: DISCRETE MODEL

The quadratic map modulated by additive period-2 forcing [14] is written as

$$x_{n+1} = f(x_n) = \lambda - x_n^2 + \alpha \cos\left(\frac{2\pi n}{2}\right). \tag{A1}$$

This map is divided into two maps as

$$x_{2n+1} = f_+(x_{2n}) = \lambda - x_{2n}^2 + \alpha, \tag{A2}$$
$$x_{2n+2} = f_-(x_{2n+1}) = \lambda - x_{2n+1}^2 - \alpha. \tag{A3}$$

We can define two maps of f_o and f_e obtained by successive alternate application of the maps f_+ and f_-:

$$x_{2n+2} = f_-[f_+(x_{2n})] \equiv f_e(x_{2n}; \lambda, \alpha), \tag{A4}$$
$$x_{2n+3} = f_+[f_-(x_{2n+1})] \equiv f_o(x_{2n+1}; \lambda, \alpha). \tag{A5}$$

If x_e^* is a fixed point of f_e then $f_+(x_e^*)$ should be a fixed point of f_o. Therefore we can infer the properties of f_o from the properties of f_e, and vice versa.

Now we consider the properties of f_e at the threshold of the period-doubling bifurcation. At the threshold,

$$f_e(x_e^*; \lambda^*, \alpha) = x_e^*, \tag{A6}$$

$$\frac{df_e}{dx}(x_e^*; \lambda^*, \alpha) = -1, \tag{A7}$$

are satisfied, where x_e^* and λ^* are the fixed point and the threshold value of the parameter, respectively.

In the absence of modulation ($\alpha = 0$ so $f_e \equiv f_o$), we can solve Eqs. (A6) and (A7), and obtain that the fixed points ($x_{0\pm}^*$) are $\frac{1\pm\sqrt{2}}{2}$ and the value of the parameter (λ_0^*) is 5/4.

In the presence of a modulation of small amplitude, α, we can treat the modulation as a perturbation and expand the fixed point and the threshold value in a series of α around their unperturbed values. When x_e^* is close to x_{0+}^*, we obtain

$$x_e^* = x_{0+}^* + \frac{1+\sqrt{2}}{2}\alpha + O(\alpha^2), \tag{A8}$$

$$x_o^* = x_{0-}^* - \frac{1-\sqrt{2}}{2}\alpha + O(\alpha^2), \tag{A9}$$

$$\lambda^* = \lambda_0^* + \frac{3\sqrt{2}}{2}\alpha + O(\alpha^2). \tag{A10}$$

So the value of the parameter at the threshold changes with α as $\lambda^* = \lambda_0^* - \frac{3\sqrt{2}}{2}\alpha$ in this case.

Similarly,

$$x_e^* = x_{0-}^* + \frac{1-\sqrt{2}}{2}\alpha + O(\alpha^2), \tag{A11}$$

$$x_o^* = x_{0+}^* - \frac{1+\sqrt{2}}{2}\alpha + O(\alpha^2), \tag{A12}$$

$$\lambda^* = \lambda_0^* - \frac{3\sqrt{2}}{2}\alpha + O(\alpha^2), \tag{A13}$$

when x_o^* is close to x_{0+}^*.

We can conclude as follows. (1) By comparing Eq. (A10) with Eq. (A13), the threshold of the period-doubling shifts in two ways. (2) By comparing Eq. (A8) with Eq. (A11), the phase difference between two branches is π. (3) The shift of the threshold is linearly dependent on the modulation amplitude.

For periodic windows with a longer period, the calculations are much more complicated, but the numerical calculations show the same features.

[1] E. Ott, C. Grebogi, and J. A. Yorke, Phys. Rev. Lett. **64**, 1196 (1990).
[2] E. R. Hunt, Phys. Rev. Lett. **67**, 1953 (1991).
[3] R. Lima and M. Pettini, Phys. Rev. A **41**, 726 (1990).
[4] Y. Braiman and I. Goldhirsch, Phys. Rev. Lett. **66**, 2545 (1991).
[5] L. Fronzoni, M. Giocondo, and M. Pettini, Phys. Rev. A **43**, 6483 (1991).
[6] R. Meucci, W. Gadomski, M. Ciofini, and F. T. Arecchi, Phys. Rev. E **49**, 2528 (1994).
[7] J. Dupré, F. Meyer, and C. Meyer, Rev. Phys. Appl. **10**, 285 (1975); W. Kreiner, IEEE J. Quantum Electron. **QE-12**, 16 (1976); E. Arimondo, F. Casagrande, L. A. Lugiato, and P. Glorieux, Appl. Phys. B **30**, 57 (1983); J. Heppner, Z. Šolajić, and G. Merkle, *ibid.* **35**, 77 (1984).
[8] M. Tachikawa, F. -L. Hong, K. Tanii, and T. Shimizu, Phys. Rev. Lett. **60**, 2266 (1988).
[9] M. Tachikawa, K. Tanii, and T. Shimizu, J. Opt. Soc. Am. B **4**, 387 (1987).
[10] M. Tachikawa, K. Tanii, M. Kajita, and T. Shimizu,

Appl. Phys. B **39**, 83 (1986), and references therein.
[11] M. Tachikawa, K. Tanii, and T. Shimizu, J. Opt. Soc. Am. B **5**, 1077 (1988); T. Sugawara, M. Tachikawa, T. Tsukamoto, and T. Shimizu, Phys. Rev. Lett. **72**, 3502 (1994); Y. Liu, P. C. de Oliveira, M. B. Danailon, and J. R. Rios Leite, Phys. Rev. A **50**, 3464 (1994).
[12] W. Gordy and R. L. Cook, *Microwave Molecular Spectra* (John Wiley and Sons, New York, 1970); B. M. Landsberg, D. Crocker, and R. J. Butcher, J. Mol. Spectrosc. **92**, 67 (1982).
[13] G. Cicogna and L. Fronzoni, Phys. Rev. E **47**, 4585 (1993).
[14] Sanju and V. S. Varma, Phys. Rev. E **48**, 1670 (1993).